Chinese Chemical Letters 34 (2023) 107954

Contents lists available at ScienceDirect

Chinese Chemical Letters

journal homepage: www.elsevier.com/locate/cclet

One-pot synthesis of Fe_xO_y nanoparticles embedded within N-doped carbon layers as highly efficient and selective catalysts for the hydrogenation of nitroarenes

Xiuzheng Zhuang[a,1], Ke Jin[b,1], Qi Zhang[a], Jianguo Liu[a], Xinghua Zhang[a], Hao Zhan[c], Longlong Ma[a,*]

[a] Key Laboratory of Energy Thermal Conversion and Control of Ministry of Education, School of Energy and Environment, Southeast University, Nanjing 210096, China
[b] Key Laboratory of Renewable Energy, Guangzhou Institute of Energy Conversion, Chinese Academy of Sciences, Guangzhou 510640, China
[c] School of Energy Science and Engineering, Central South University, Changsha 410083, China

ARTICLE INFO

Article history:
Received 8 August 2022
Revised 10 October 2022
Accepted 23 October 2022
Available online 27 October 2022

Keywords:
Facile synthesis
Iron-based catalyst
Carbonaceous layers
Nitroarenes reduction

ABSTRACT

Inhibiting the side reactions while promoting hydrogenation are the main target for the production of functional anilines from nitroarenes; consequently, the preparation of an ideal catalyst to improve chemical selectivity is one of the hot issues. In this work, we provided an easy-to-prepare catalyst with N-doped carbon layers, where the FexOy nanoparticles were encapsulated and distributed uniformly. The structural features of catalyst were characterized by several techniques, and the selected catalyst was next applied to the hydrogenation of nitrobenzene under varied conditions, involving temperature, holding period and H2 pressure. Subsequently, we conducted the synthesis of more than 16 substrates for the corresponding anilines with varied functional groups. The hydrogenation protocol to gram-scale synthesis as well as lifecycle performance were also demonstrated in the batch reactor, together with the explanation of its catalytic mechanisms. Overall, the present work provides an available preparation of simple but highly efficient catalysts for the production or aromatic amines, which will be benefit for the sustainable development of this field in near future.

The selective hydrogenation of nitroarenes into corresponding anilines is one of the essential routes in organic synthesis, which is widely used in the production of agrochemicals, pharmaceuticals and dyestuffs [1,2]. In the traditional industry, functionalized anilines are commonly obtained through several methods including chemical reagent reduction [2,3] as well as catalytic hydrogenation reduction [4,5]. Among them, the latter has attracted considerable attentions recently as its advantages in terms of efficiency, safety and sustainability. Green chemistry is being called upon as a result of the increasingly strict environmental requirements in today's industry. Accordingly, lots of efforts have been made to develop potential catalysts for its scale application, but the inferior chemoselectivity in catalytic system is still the challenge because of the strong adsorption of intermediate products towards catalysts [5], which increase the difficulty of selective hydrogenation of substituents on nitroarenes with other reducible or halogenated groups. More importantly, nitroarene hydrogenation presents a complex reaction network containing many intermediates or by-products [3,6], such as nitroso derivatives, hydroxylamines, and azocompounds; so, the inhibition of effective adsorption or side reaction is the technical problems to achieving excellent selectivity in the hydrogenation of nitroarenes.

Most of the relevant studies on producing aromatic amines is heavily dependent on precious metals, such as Pd/Mo_2C [7] and Ru/SiO_2 [8], which performs great catalytic conversion yet at the expense of over hydrogenation and undesired dehalogenation. The substitution of costly precious-metal catalysts with non-noble one holds enormous promise, and some of them have been successfully developed in lab scale, especially for the iron oxide with nanostructure. For instance, Papadas *et al.* [9] prepared the g-Fe_2O_3 mesoporous nanoparticles which performed well in the hydrogenation of nitroarenes as its tolerance to halogenated groups, while similar achievement was observed by employing flower-like micro-mesoporous iron oxide as catalyst [10]; unfortunately, both of them required relatively harsh conditions. Soon after, a Fe_2O_3@N-doped carbon materials had been reported by Feng *et al.* [11], Xu *et al.*

* Corresponding author.
E-mail address: mall@seu.edu.cn (L. Ma).
[1] These authors contributed equally to this work.

https://doi.org/10.1016/j.cclet.2022.107954
1001-8417/

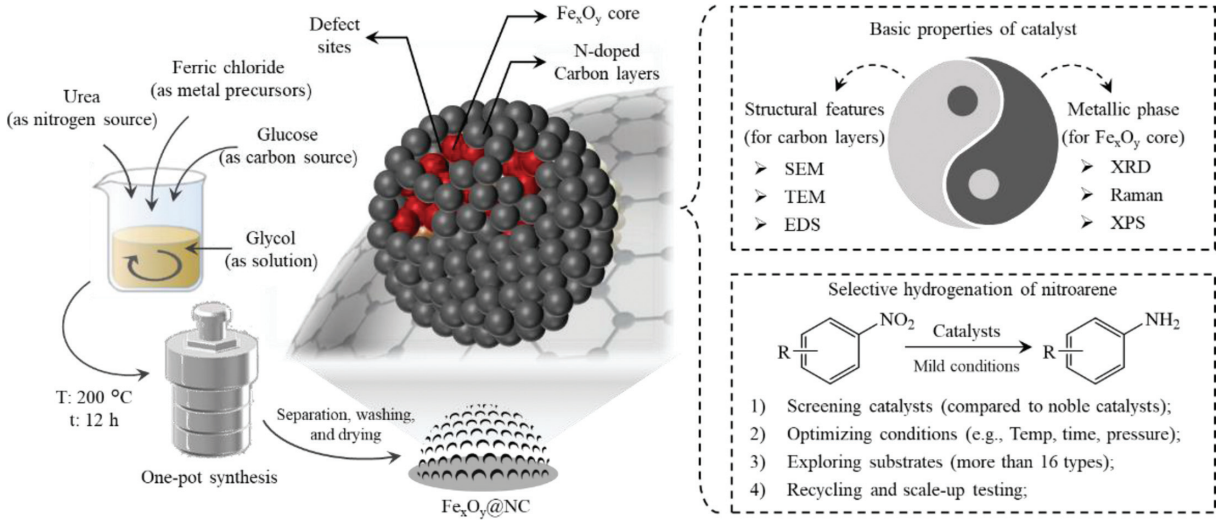

Fig. 1. The preparation of metallic nanoparticles and its subsequent application.

[12], and Zou *et al.* [6], who claimed that the iron oxide nanoparticles covered by carbon layers are the active species for selective hydrogenation of nitroarenes. Zou *et al.* [6] also found that oxygen vacancies in iron oxide lead to the lattice distortion, which contributes to the hydrogenation of nitroarenes but its specific mechanisms are still confused, reflecting that there is still a long way to fully understand the interplay between carbon layer and iron oxide. Not only that, the addition of nitrogen into carbon layers exhibits an improvement on the catalytic activity, drawing another scientific problem associated with the correlations between carbon layer, nitrogen atom and metallic nanoparticles [12–14]. Consequently, to fabricate nanostructure catalysts in an effective route is highly desirable, which can not only promote the hydrogenation of nitroarene in relatively mild reaction conditions, but also help to reveal the catalytic mechanisms and specific relationship of each composition.

In the present work, we developed a simplified method for the preparation of Fe_xO_y nanoparticles coated by the N-doped carbon layers (Fe_xO_y@NC) in one-pot synthesis, where the experimental procedure and the subsequent application are depicted in Fig. 1. Generally speaking, the iron oxides in this catalytic system are decorated with layers of N-doped carbon that derived from the hydrothermal processes of glucose (as carbon source) and urea (mostly as nitrogen source); so, the formation of carbonaceous supports and the combination of metallic oxides are occurred concurrently. In addition, the thickness and porosity of N-doped carbon layers can be adjusted by varying the usage of glucose during hydrothermal carbonization, thereby controlling the catalytic properties of catalyst and exhibiting new insights in the processing mechanism. Thus, several techniques are employed to analyze the basic properties of catalysts (named as Fe_xO_y@NC-x, where "x" represents the usage of glucose), following by the selective hydrogenation of nitroarenes.

First of all, the surface morphology and metal distribution of catalysts were analyzed *via* SEM, TEM and EDS, whose results were summarized in Fig. 2 (took Fe_xO_y@NC-0.2g as an example). As can be seen, a large number of carbon microspheres with hollow core were formed and equably dispersed during the hydrothermal processes, and its magnified image gave the evidence of porosity by showing obvious channels through the internal and external. Both of them can provide abundant active sites and satisfied contact area between metallic phase and aqueous reactant, thus improving catalytic activity and the corresponding kinetics [15]. The TEM results also indicated that metallic nanoparticles with sizes of 3.7–9.3 nm (average: 6.6 nm) were coated by the outer layers (~2.4 nm) with lattice fringes of 0.33 nm [11,15], assigning to (002) plant of graphitic carbon. This situation is in contrast to the lattice fringes of the nanoparticles themselves at 0.48 nm, which corresponds to the (111) plane of iron oxides [16]. Additionally, the elemental mapping provided direct evidence that the carbon layers are incorporated with nitrogen while the metallic atoms are well distributed within the N-doped carbon layers. Li *et al.* [4] and Wu *et al.* [5] believed that the combination between metal atoms and carbon layer may be caused by their cooperation during the formation and growth of crystal nucleus. Benefited from that, the carbon layers can serve as a protective shell to effectively impede the metallic nanoparticles from agglomeration and leaching, which ensures that the active sites are highly stable and durable when used in the aqueous systems [15,17,18]. At the meanwhile, the addition of nitrogen may offer synergistic functions during catalytic processes based on previous studies [11,12,17]. However, by varying the amount of glucose, the structural features were significantly changed, and the catalytic properties may be accordingly affected to a large extent. It can be observed in Fig. S1 (Supporting information) that only the carbon in urea barely forms the carbon layers (Fe_xO_y@NC-0g), which is not easily to function as a catalyst because most of metallic nanoparticles are not successfully loaded during preparation. On the contrary, the over use of glucose will cause the defect-free carbon layers (Fe_xO_y@NC-0.4g in Fig. S2 in Supporting information), leading to the complete encapsulation of metallic nanoparticles which may cut the connection between aqueous reactant and metallic phase.

Subsequently, the XRD patterns of the prepared catalysts are exhibited in Fig. 3a, where the metallic state in Fe_xO_y@NC with glucose addition less than 0.4 g were all attributed to the F_3O_4 phase (JCPDS 88-0315), corresponding to the diffraction peaks at 30.2°, 35.4°, 42.5°, 57.2°, and 62.7°. According to previous literatures [15,19], this situation can be explained by the interaction between urea, Fe^{3+} and glycol. During the hydrothermal synthesis, urea is easily decomposed and produce OH^- ions in the aqueous system, which will connect with Fe^{3+} to form the intermediate such as $Fe(OH)_3$; after that, the glycol can reduce these intermediates into $Fe(OH)_2$ which can function as the crystal nucleus. Following with the accumulation of crystal nucleus, H^+ ions are insufficient and the dehydration of intermediates become predominant, thereby forming metallic Fe_3O_4 at the end of hydrothermal process. Li *et al.* [4] also mentioned that the peaks in 42.5° may be associated with FeN_x species, which is probably due to the

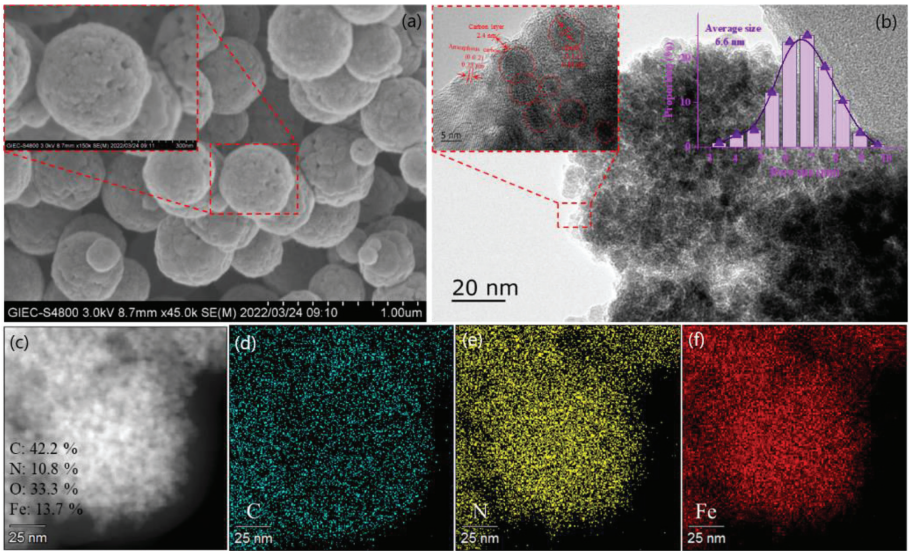

Fig. 2. The SEM (a), TEM (b) and EDS (c–f) results of Fe_xO_y@NC-0.2g catalyst.

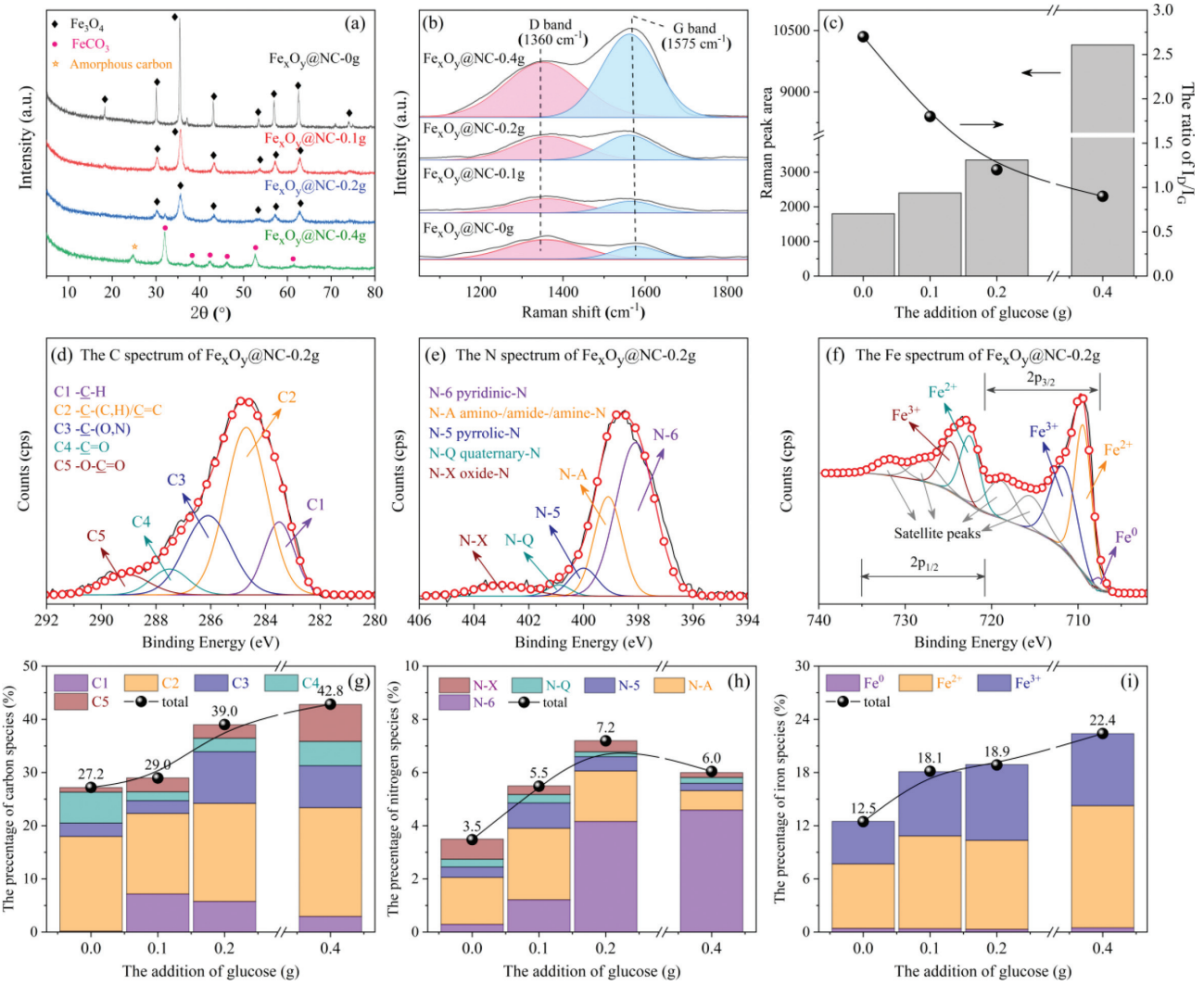

Fig. 3. The XRD (a), Raman (b, c) and XPS (d–i) results of Fe_xO_y@NC catalysts. Note: The percentage of C, N, and Fe in Figs. 3g–i were obtained from the semi-quantitative analysis of XPS, and the percentage of Fe species in Fig. 3i was only calculated from $2p_{3/2}$.

Fe-N interaction on the surface of Fe_3O_4 nanoparticles. However, the intensity of Fe_3O_4 phase was gradually weakened if keep on adding glucose, and the main state of metallic phase finally turned to $FeCO_3$ in Fe_xO_y@NC-0.4g, which is caused by the increased release of CO_2 during the hydrolysis of carbon source [18]. On the other hand, the Raman spectroscopy was established as a unique tool in probing the microstructure of catalysts based on the structural parameters calculated from the XRD results [20,21]. It can be seen in Fig. 3b that the D band (at 1360 cm^{-1}) and G band (at 1580 cm^{-1}) can be obviously observed in all samples, and the processing parameters are accordingly calculated in Fig. 3c. The total peak area in the region of 1800–1000 cm^{-1} represents the overall intensity for the corresponding Raman spectrum, which keeps on increasing with the addition of glucose, illustrating the accumulation of electron-rich functional groups on the particle surface that will improve the Raman scattering ability [21]. Besides, the decrease of I_D/I_G suggests that the carbon layers in the catalysts are more graphitic [12,15], which is also ascribed to the gradual addition of glucose.

In addition to the XRD and Raman, the chemical valence of specific atoms in Fe_xO_y@NC-0.2g was further investigated by XPS [4,15,19], including C, N, and Fe species whose spectra were shown in Figs. 3d–f, respectively, together with their variation in different conditions (Figs. 3g–i). The carbon content on the surface of catalysts grew with the amount of glucose, and most of them existed in the form of -C-(C, H)/C=C. However, the rest of carbon cooperated with oxygen and nitrogen atoms significantly increased from 9.2% (at Fe_xO_y@NC-0g) to 19.4% (at Fe_xO_y@NC-0.4g), coinciding well with the Raman results, which indicates that adding glucose can provide more sites for heteroatom to enrich the surface functionalities [12]. Similarly, the percentage of N-A, which originated from the urea, reduced while the other connected with aromatic carbon such as N-5, N-6 and N-X were steadily obvious with the increasing amount of glucose. Xia *et al.* [15] also stated that the peaks of N-5 and N-6 reflects the existence of metal-N interactions. Meanwhile, the N-6 peak at Fe_xO_y@NC-0g (located at 398.2 eV) was positively shifted to 398.7 eV in Fe_xO_y@NC-0.4g (as shown in Fig. S3 in Supporting information), which is possibly contributed by an improvement in the oxidation state of nitrogen caused by Fe-N bond formation [12,15]. This situation suggests abundant nitrogen was successfully doped into carbon and metallic functionalities during hydrothermal synthesis, which can provide additional active centers for catalytic processes. As for the Fe 2p spectra, a very slight peak corresponding to Fe^0 (at 707.1 eV) was observed, but that of Fe^{2+} and Fe^{3+} occupied the dominant situation at 709.8 eV and 711.2 eV, respectively, indicating that the iron oxides are the main forms in the prepared catalysts [19]. The peaks of iron oxide between $2p_{3/2}$ and $2p_{1/2}$ were correlated in a gap of 13.6 eV, and the satellite peaks were followed with the corresponding peaks, which is consistent with the typical profiles of metallic irons [4,19].

Regarding to the catalytic activity, the selective hydrogenation of nitroarenes based on these catalysts was carried out to explore and correlate the catalytic performance with observed changes in sample properties [5,6,10,12,14]. As can be seen in Table 1, entries 1–4 exhibited the hydrogenation of nitrobenzene over a series of prepared catalysts with different amount of glucose, which suggests that the Fe_xO_y@NC-0.2g is the best because of its excellent conversion and selectivity reaching at >99% and 94.6%, respectively. In contrast, adding excessive glucose (*i.e.*, 0.4 g) during the hydrothermal processes might lead to the pore-free layers which hinders the effective contact between aqueous reactant and metallic phase, whereas less amount of glucose (*e.g.*, 0 g or 0.1 g) is insufficient to form the carbon layers. Both of them are detrimental to the catalytic processes, and the similar findings are also reported by Xu *et al.* [12] and Zuo *et al.* [6] in 2016 and 2018, respectively.

Table 1
Selection hydrogenation of nitrobenzene over different catalysts and conditions.[a]

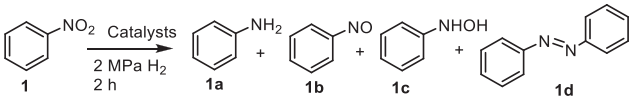

Entry	Catalysts (mg)	Conv. (%)	Yield of **1a** (%)[b]
1	Fe_xO_y@NC-0g (10)	2.8	0.2
2	Fe_xO_y@NC-0.1g (10)	9.5	5.4
3	Fe_xO_y@NC-0.2g (10)	>99	94.6
4	Fe_xO_y@NC-0.4g (10)	42.6	29.5
5	Carbon microspheres (10)	13.1	4.2
6	5% Ru/C (10)	>99	21.8
7	5% Pt/C (10)	>99	94.1
8	5% Rh/C (10)	>99	1.7
9	5% Pd/C (10)	>99	80.1
10	Fe powder (10)	22.2	0.8
11	Fe_3O_4 (10)	>99	91.3
12	Fe_xO_y@NC-0.2g (10)	18.7 [c]	1.2
13	Fe_xO_y@NC-0.2g (10)	63.1 [d]	37.0
14	Fe_xO_y@NC-0.2g (5)	58.4	50.0
15	Fe_xO_y@NC-0.2g (10)	67.6 [e]	54.9
16	Fe_xO_y@NC-0.2g (10)	59.2 [f]	46.2

[a] The screening of prepared and commercial catalysts was based on the below conditions: 80 °C, 2 h, 5 mL MeOH, 2 MPa H_2, and 0.5 mmol nitrobenzene.
[b] Yield of **1a** was determined by GC-MS and ^1H NMR spectroscopy using 1,3,5-trimethoxybenzenen as an internal standard.
[c] Reaction temperature is 60 °C.
[d] Reaction temperature is 70 °C.
[e] Reaction time is 1 h.
[f] Reaction pressure is 1 MPa H_2.

Meanwhile, the catalytic activity of Fe_xO_y@NC-0.2g is comparable, or even superior, to most of commercial catalysts, such as 5% Ru/C (entry 6), 5% Pt/C (entry 7), 5% Rh/C (entry 8), and 5% Pd/C (entry 9). In order to identify which component functioning as the active sites, the entry 5 was used as the contrast sample, indicating that only carbon layers will barely affect the hydrogenation. The entries 10 and 11 reflected that Fe_3O_4 can catalyze nitrobenzene into aniline with a satisfied yield; by combining with its featural analysis, it can be concluded that the Fe_3O_4 is the main valence state in Fe_xO_y@NC-0.2g which plays the most important part in catalyzing selective hydrogenation. More interestingly, the better performance caused by Fe_xO_y@NC-0.2g than pure Fe_3O_4 also implied that there is a synergistic effect resulted from the N-doped carbon layer. This phenomenon is in accordance with previous literatures which indicated that the dope of nitrogen near carbon atoms might induce a high positive charge density, thereby improving the adsorption of compounds containing nitro groups [11,18].

Based on the above results, the selective hydrogenation of nitrobenzene can be successfully done by the Fe_xO_y@NC-0.2g, and the optimization of reaction conditions involving temperature, time, H_2 pressure, and the amount of catalyst was further evaluated [17,20]. Obviously, higher temperature facilitated the hydrogenation of nitrobenzene, steadily increasing the yield of **1a** from 21.8% at 60 °C (entry 12) to 94.6% at 80 °C (entry 3). Similar trends could be observed for the amount of catalyst (entry 14), the holding period (entry 15), and the H_2 pressure (entry 16).

Not only that, we also explore the different sources of hydrogen and heating methods for the hydrogenation of nitroarenes [14,16]. As can be seen from the entry 1 in Table 2, only methanol could barely provide sufficient H^+ for hydrogenation, even at the severe conditions. In comparison, replacing H_2 with HCOOH (entry 2, Table 2) or $N_2H_4{\cdot}H_2O$ (entry 3, Table 2) as hydrogen source satisfied the requirement for the hydrogenation of nitrobenzene, but both of the temperature and time are still high [14]. The use of microwave heating instead of conventional method improved the yield of **1a** under relatively mild conditions [16]. However, it is still unacceptable when compared to the use of H_2 as hydrogen source

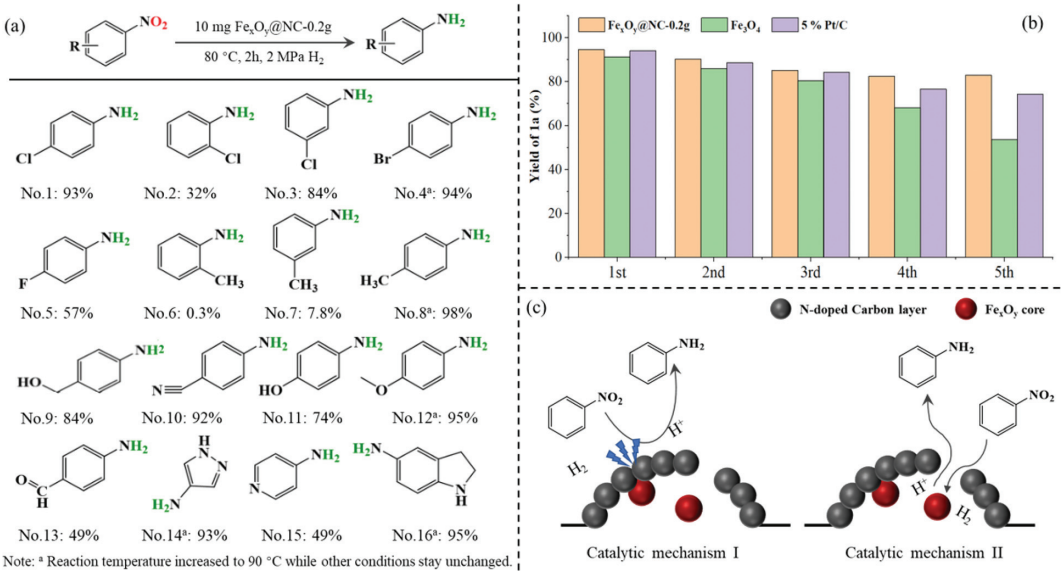

Fig. 4. (a) The selective hydrogenation of functional nitroarenes catalyzed by the Fe_xO_y@NC-0.2g; (b) The recycling test of the Fe_xO_y@NC-0.2g and commercial catalysts; (c) The catalytic mechanism of hydrogenation over the Fe_xO_y@NC-0.2g.

Table 2
Selective hydrogenation of nitrobenzene under different hydrogen sources and heating methods using Fe_xO_y@NC-0.2g (10 mg) as catalyst.[a]

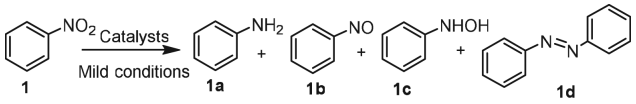

Entry	Temp (°C)	Time (h)	Hydrogen source	Conv. (%)	Yield of **1a** (%)[b]
1	150	16	Only methanol	16.8	0.4
2	90	12	2.0 mmol HCOOH	75.1	67.3
3	120	10	2.0 mmol $N_2H_4{\cdot}H_2O$	58.1	52.5
4	90	4	2.0 mmol HCOOH	68.9	54.2
5	120	4	2.0 mmol $N_2H_4{\cdot}H_2O$	80.2	78.8

[a] Entries 1–3 were heated by conventional method as usual, while entries 4 and 5 were heated by microwave method. 0.5 mmol nitrobenzene was used in this test, and methanol was used as solvent.
[b] Yield of **1a** was determined by GC-MS and ^{1}H NMR spectroscopy using 1,3,5-trimethoxybenzenen as an internal standard.

(entries 4 and 5, Table 2). Thus, the selective hydrogenation of nitrobenzene catalyzed by Fe_xO_y@NC-0.2g can reach its best result under the optimized conditions at 80 °C, 2 h, 10 mg catalysts, and 2 MPa H_2 pressure.

With the optimal conditions in hand, the general scope of the Fe_xO_y@NC-0.2g catalyst was investigated for the selective hydrogenation of halogenated or unsaturated nitrobenzene, and the result was shown in Fig. 4a. It is exciting to find that the electron withdrawing substituents, especially for Cl, Br or F, were well tolerated and had no cross reactivity to undergo competitive reduction, contrasting other noble-based catalysts that usually causes dehalogenation during the hydrogenation [13]. For instance, the 4-chloronitrobenzene (No. 1) was almost fully converted to the corresponding chloroanilines with an excellent selectivity (>99%); however, the effectiveness was affected by the space steric hindrance [20], such as Nos. 2 and 3. This phenomenon could also be observed at the series of methyl-substituted nitrobenzene, whose yield of target products followed with an order of No. 8 (98%) > No. 7 (7.8%) > No. 6 (0.3%). Notably, the No. 8 was performed at a higher temperature (*i.e.*, 90 °C), which suggests that providing more heat can help to overcome the space steric hindrance to some extent. Regarding to Nos. 4 and 5, the relatively lower yield of target product was confirmed by Cao *et al.* [13] and Pan *et al.* [22], whose found that the C-F and C-Br bonds are susceptible to the dehalogenation because of the large atomic diameter as well as the low electronegativity. In addition, some of the reducing-labile functional groups were also well tolerated in this catalytic system, such as hydroxy– (Nos. 9 and 11), nitrile- (No. 10), ether- (No. 12), aldehyde- (No. 13), and other heterocyclic groups (Nos. 14–16), affording the corresponding nitro aromatics in satisfied yields. It is also noteworthy that three substrates including nitrobenzene, 4-nitrotoluene and 4-nitroanisole were selected for the selective hydrogenation at gram-scale experiments, and all of them were similar to the small-scale reactions by exhibiting excellent yields of target products at 95%, 97% and 94%, respectively, shown in Table S1 (Supporting information).

In terms of the reusability of the prepared catalyst, we carried out the selective hydrogenation of nitrobenzene over Fe_xO_y@NC-0.2g in successive runs, and complied the results in Fig. 4b, where Fe_3O_4 and 5% Pt/C were adopted as the commercial catalysts for comparison. As can be seen, the catalytic activity of Fe_xO_y@NC-0.2g was slightly reduced at the beginning but gradually stabilized at 83% after recycling five times; by contrast, the reusability of Fe_3O_4 and 5% Pt/C were relatively inferior, reducing from 91% to 54% and 94% to 74% at the 5th cycle, respectively. This difference is possibly owing to the carbon layers in Fe_xO_y@NC-0.2g which encapsulates the metallic nanoparticles, thereby physically isolating them from leaching and aggregating at the reaction stage [12,18,20]. More interestingly, because of the magnetic property held by the Fe_xO_y core, the prepared catalyst can be easily recycled, exhibiting an attractive benefit in industrial application [12,18].

Last but not least, according to the above results, we proposed the possible mechanisms for the selective hydrogenation of nitrobenzene over Fe_xO_y@NC-0.2g, and the result was illustrated in Fig. 4c. In fact, the catalytic performance is possibly dependent on the adsorption behavior of nitroarenes on the active sites, but two possible mechanisms are involved, which may occur individually or simultaneously [9,17,23]. In simple terms, (1) the metallic nanoparticles are covered by carbon layers with defect sites, where H_2 can be diffused throughout and activated for the hydrogenation [9,17], and (2) the outer graphitic shell can be activated by the electronic interaction between inner metallic nanoparticles and outer graphene layer [23]. Both of them affect the adsorption

behavior of relevant reactants on active sites (outside or inside the carbon layers); however, the general steps of catalytic processes are similar, which can be tracked back from the previous studies [5].

In summary, we have successfully explored the catalytic performance of Fe_xO_y@NC-0.2g on the selective hydrogenation of nitroarenes, which indicates that a wide scope of substrates are well tolerated under mild conditions. This protocol also exhibited a similar reactivity during the gram-scale and recycling tests without any significant loss of catalytic activity. More specifically. the superior of Fe_xO_y@NC-0.2g in catalytic activity and stability mainly originates from the Fe_3O_4 core protected by the N-doped carbon layers, where nitrogen atoms induce synergetic effects between carbonaceous matrix and metallic phase. The above findings strongly confirm an available and feasible preparation of simple but highly efficient catalysts for the selective hydrogenation of nitro aromatics. By and large, the advantages of this newly developed and simplified method are recommended for the synthesis of functional anilines, as well as the highly efficient and industrial applicable tandem synthesis process.

Declaration of competing interest

The authors declare no conflict of interest.

Acknowledgments

This work was supported financially by the National Natural Science Foundation of China (Nos. 52236010, 51876209, 51876210 and 51906247) and the Fundamental Research Funds for the Central Universities (No. 2242022R10058).

References

[1] G. Purohit, D.S. Rawat, O. Reiser, ChemCatChem 12 (2020) 569–575.
[2] S. Tadrent, A. Khelfa, C. Len, Sustainability 12 (2020) 4665.
[3] B.N. Zhao, Z.P. Dong, Q.Y. Wang, et al., Nanomaterials 10 (2020) 883.
[4] J. Li, J.L. Liu, H.J. Zhou, Y. Fu, ChemSusChem 9 (2016) 1339–1347.
[5] W. Wu, W. Zhang, Y. Long, J.H. Qin, J.T. Ma, Mol. Catal. 497 (2020) 10.
[6] P.P. Zuo, J.Q. Duan, H.L. Fan, S.J. Qu, W.Z. Shen, Appl. Surf. Sci. 435 (2018) 1020–1028.
[7] W.J. Song, X.D. Yi, X.M. Jiang, W.K. Lai, Ind. Eng. Chem. Res. 59 (2020) 20298–20306.
[8] X.J. Cui, F. Shi, Y.Q. Deng, ChemCatChem 4 (2012) 333–336.
[9] I.T. Papadas, S. Fountoulaki, I.N. Lykakis, G.S. Armatas, Chem. Eur. J. 22 (2016) 4600–4607.
[10] Y.S. Ma, L.Y. Zhang, W. Shi, et al., Chin. Chem. Lett. 30 (2019) 183–186.
[11] B.B. Feng, Q.H. Xu, X.X. Wu, et al., Appl. Surf. Sci. 557 (2021) 149837.
[12] S.D. Xu, D.Q. Yu, S.F. Liao, T. Ye, H.D. Sheng, RSC Adv. 6 (2016) 96431–96435.
[13] Y.L. Cao, K.K. Liu, C. Wu, H.P. Zhang, Q.Y. Zhang, Appl. Catal. Gen. 592 (2020) 9.
[14] S.B. Tian, M. Hu, Q. Xu, et al., Sci. China Mater. 64 (2021) 642–650.
[15] S.W. Xia, W.H. Guo, N. Cai, et al., Fuel Process. Technol. 224 (2021) 107028.
[16] M. Manzoli, E.C. Gaudino, G. Cravotto, et al., ACS Sustain. Chem. Eng. 7 (2019) 5963–5974.
[17] T. Stemmler, A.E. Surkus, M.M. Pohl, K. Junge, M. Beller, ChemSusChem 7 (2014) 3012–3016.
[18] J.L. Tu, J.J. Yuan, S.M. Kang, Y.J. Xu, T.J. Wang, New J. Chem. 42 (2018) 10861–10867.
[19] J.X. Wang, S.P. Zhang, Y.H. Su, S.G. Zhu, Fuel 305 (2021) 121552.
[20] X.Z. Zhuang, J.G. Liu, S.R. Zhong, L.L. Ma, Green Chem. 24 (2022) 271–284.
[21] X.Z. Zhuang, H. Zhan, Y.P. Song, et al., Fuel 236 (2019) 960–974.
[22] H.J. Pan, Y.Y. Peng, X.H. Lu, et al., Mol. Catal. 485 (2020) 9.
[23] L. Yu, D.H. Deng, X.H. Bao, Angew. Chem. Int. Ed. 59 (2020) 15294–15297.